www.nature.com/aps

Acta Pharmacologica Sinica

ARTICLE

Probiotics protect against RSV infection by modulating the microbiota-alveolar-macrophage axis

Jian-jian Ji[1], Qin-mei Sun[2], Deng-yun Nie[3], Qian Wang[4], Han Zhang[2], Fen-fen Qin[3], Qi-sheng Wang[2], Sheng-feng Lu[5], Guo-ming Pang[6] and Zhi-gang Lu[2,4,5,6]

Respiratory syncytial virus (RSV) is leading cause of respiratory tract infections in early childhood. Gut microbiota is closely related with the pulmonary antiviral immunity. Recent evidence shows that gut dysbiosis is involved in the pathogenesis of RSV infection. Therefore; pharmacological and therapeutic strategies aiming to readjust the gut dysbiosis are increasingly important for the treatment of RSV infection. In this study, we evaluated the therapeutic effects of a probiotic mixture on RSV-infected mice. This probiotic mixture consisted of *Lactobacillus rhamnosus GG, Escherichia coli Nissle 1917* and *VSL#3* was orally administered to neonatal mice on a daily basis either for 1 week in advance or for 3 days starting from the day of RSV infection. We showed that administration of the probiotics protected against RSV-induced lung pathology by suppressing RSV infection and exerting an antiviral response via alveolar macrophage (AM)-derived IFN-β. Furthermore, administration of the probiotics reversed gut dysbiosis and significantly increased the abundance of short-chain fatty acid (SCFA)-producing bacteria in RSV-infected mice, which consequently led to elevated serum SCFA levels. Moreover, administration of the probiotics restored lung microbiota in RSV-infected mice. We demonstrated that the increased production of IFN-β in AMs was attributed to the increased acetate in circulation and the levels of *Corynebacterium* and *Lactobacillus* in lungs. In conclusion, we reveal that probiotics protect against RSV infection in neonatal mice through a microbiota-AM axis, suggesting that the probiotics may be a promising candidate to prevent and treat RSV infection, and deserve more research and development in future.

Keywords: respiratory syncytial virus; probiotics; gut microbiota; lung microbiota; alveolar macrophages; SCFAs

Acta Pharmacologica Sinica (2021) 42:1630–1641; https://doi.org/10.1038/s41401-020-00573-5

INTRODUCTION

Respiratory syncytial virus (RSV) is a negative sense, single-stranded RNA virus, and RSV infection is a leading cause of acute respiratory tract infection in early childhood [1]. Recent studies have shown that gut dysbiosis is critically involved in the pathogenesis of RSV infection; [2] therefore, pharmacological and therapeutic strategies aiming to readjust the gut microbiota are becoming increasingly popular for the treatment of RSV infection.

The gut microbiota plays many critical roles in maintaining human health [3]. Respiratory viral infection, such as influenza and RSV infections, can induce gut dysbiosis. In RSV infection, it has been reported that the composition and diversity of gut microbiota are profoundly altered [2, 4]. Gut dysbiosis is closely related to pulmonary immune dysfunction in respiratory viral infection [5, 6]. There is emerging evidence that the gut microbiota plays a role in modulating the lung immune response in respiratory viral infection [4, 7]. For example, infection with influenza dampens the bactericidal activity of alveolar macrophages (AMs) through gut microbiota-derived short-chain fatty acids (SCFAs) [4], and antibiotic-driven gut microbiome perturbation alters lung antiviral immunity in humans during influenza infection [8]. The gut microbiota has been shown to influence pulmonary immunity through what is commonly referred to as the gut–lung axis [7]. The gut microbiota can generate metabolites that alter the function of immune cells in the lungs, such as SCFAs and indoles, which have many effects, including regulating immune function [9].

A previous study showed that commensal bacteria calibrated the activation threshold of lung innate antiviral immunity [10]. Several studies have revealed that the antiviral effects of the gut microbiota are dependent on inducing type I interferon (IFN) production [10, 11], and antibiotic-treated mice and germ-free (GF) mice have an impaired ability to produce IFNβ [12]. A recent study showed that the gut microbiota-mediated upregulation of the expression of type I IFNs might occur through acetate and indoles, and acetate and indoles could promote the activation of the IFNβ response [13, 14]. Moreover, butyrate suppresses influenza infection through the enhanced generation of Ly6c-patrolling monocytes and boosts $CD8^+$ T cell effector function [15]. Mice fed

[1]Jiangsu Key Laboratory of Pediatric Respiratory Disease, Institute of Pediatrics, Nanjing University of Chinese Medicine, Nanjing 210023, China; [2]The First School of Clinical Medicine, Nanjing University of Chinese Medicine, Nanjing 210023, China; [3]College of Pharmacy, Nanjing University of Chinese Medicine, Nanjing 210023, China; [4]International Education College, Nanjing University of Chinese Medicine, Nanjing 210000, China; [5]Key Laboratory of Acupuncture and Medicine Research of Ministry of Education, Nanjing University of Chinese Medicine, Nanjing 210023, China and [6]Kaifeng Hospital of Traditional Chinese Medicine, Kaifeng 475000, China
Correspondence: Zhi-gang Lu (luzg@njucm.edu.cn) or Guo-ming Pang (kfszyypgm@163.com)
These authors contributed equally: Jian-jian Ji, Qin-mei Sun

Received: 8 July 2020 Accepted: 4 November 2020
Published online: 25 January 2021

SCFAs or a diet high in fermentable fiber had decreased lung damage and viral load and increased survival during influenza and RSV infections [13, 15]. Thus, gut microbiota-derived metabolites provide protective roles in respiratory viral infection. Modulating virus-induced gut dysbiosis using probiotics or faecal microbiota transplantation-based interventions might confer protection against viral infections [16].

Recent studies have found that the respiratory tract harbors a microbial community, which plays an important role in defending against pathogenic infection and modulating the immune system [17, 18]. The lung microbiota can modulate immune responses against viral infection [17, 19], and dysregulation of the lung microbiota significantly affects the host's immune ability to defend against pathogens [20–22]. In terms of the protective role of lung microbiota in lung immunity, the intranasal administration of probiotics, such as *Corynebacterium* and *Lactobacillus*, was shown to promote macrophage secretion of IFN-β, suppressing RSV infection [23]. Thus, targeting the lung microbiome might also provide a novel and promising treatment for RSV infection.

Probiotics are live microorganisms and one of the most widely accepted strategies to modulate the gut microbiota and normalize dysbiosis [24]. Multiple studies suggest that probiotics are beneficial for several human diseases, including respiratory infectious diseases, obesity, and diabetes [25]. Several studies indicate that probiotic supplementation can prevent influenza infection by regulating the gut microbiota [16, 26]. Thus, modulating gut dysbiosis using probiotics might provide a promising treatment strategy for RSV infection. A previous study showed that treatment with *Lactobacillus rhamnosus GG (LGG)* considerably improved neonatal mouse survival after influenza virus infection by upregulating type I IFN pathways [27]. *Escherichia coli Nissle 1917 (ECN)* can defend against *rotavirus* infection by increasing levels of IFN-α [28]. VSL#3 can also increase anti-*Candida* defenses by promoting IFN-α release [29]. These studies indicated that *LGG, ESN,* and *VSL#3* might potentially restrict viral infection by modulating type I IFN pathways. A previous study demonstrated that a probiotic mixture, which consisted of *LGG, ESN*, and *VSL#3*, was effective in modulating gut dysbiosis and suppressed hepatocellular carcinoma growth in mice [30]. The intake of this preventive probiotic mixture drastically increased the metabolic potential of SCFA (acetate and propionate) production and enhanced anti-inflammatory activities in mice [30]. Collectively, based on these previous studies, we speculate that the probiotic mixture may be effective in restoring RSV infection-induced gut dysbiosis and defending against RSV infection. Therefore, we explored the effects of this probiotic mixture on gut dysbiosis and protecting against RSV infection in RSV-infected mice. Our study may provide evidence for a new therapeutic strategy for RSV infection.

MATERIALS AND METHODS

Reagents and antibodies

Company (Gaithersburg, MD, USA). *ECN* was purchased from Bioprox (France). Vancomycin, neomycin, ampicillin, and metronidazole were purchased from Sigma-Aldrich (St. Louis, MO, USA). A myeloperoxidase assay kit was purchased from Nanjing Jiancheng Bioengineering Institute (Nanjing, China). The Mouse Albumin ELISA Quantitation Set was purchased from Bethyl Laboratories (Montgomery, TX, USA). Clodronate liposomes were purchased from Roche Diagnostics (Mannheim, Germany). Rabbit polyclonal antibodies against phospho-IRF3-PE (Ser396, #29047), phospho-TBK1 (Ser172, #5483), and IFNβ (#97450 s) were purchased from Cell Signaling Technology (Danvers, MA, USA). The IFNβ ELISA Kit was purchased from PBL Assay Science (Piscataway, NJ, USA). RSV fusion protein antibody was purchased from Santa Cruz Biotechnology (#sc-101362). SYBR Green PCR Master Mix was purchased from Applied Biosystems (Foster City, CA, USA). Dulbecco's modified Eagle's medium, RPMI-1640 medium and fetal bovine serum (FBS) were purchased from Gibco Invitrogen (Paisley, UK). Human RSV strain A2 was purchased from Wuhan University Virus Institute (Wuhan, China).

Probiotics

The probiotics used in this study were according to those in a previous study [30]. The new probiotic combination consisted of *LGG, viable Escherichia coli Nissle 1917 (EcN)*, and heat-inactivated *VSL#3* (1:1:1). VSL#3 was provided by VSL Pharmaceutical Company and contains *Streptococcus thermophilus*, *Bifidobacterium breve*, *Bifidobacterium longum*, *Bifidobacterium infantis, Lactobacillus acidophilus, Lactobacillus plantarum, Lactobacillus paracasei* and *Lactobacillus delbrueckii subspecies*. *Lactobacillus rhamnosus strain GG (KP-GG 400B)* was supplied by Danisco, each containing more than 5×10^9 colony-forming units. Mutaflor capsules containing $(2.5–25) \times 10^9$ nonpathogenic *E. coli Nissle 1917 (ECN)* strain were used.

In vivo studies

Six-week-old female BALB/c mice (SPF grade) were obtained from the Model Animal Research Center of Nanjing University (Nanjing, China) and kept under pathogen-free housing conditions in a 12-h light and dark cycle. All experimental procedures were performed in accordance with the National Institutes of Health Guidelines for Laboratory Animals and approved by the Animal Ethics Committee of Nanjing University of Chinese Medicine (Permission Number: ACU-29(20161230)). The mice were randomized into 5 groups ($n = 8$ per group): (i) probiotic-treated mice, with the dose of probiotics according to that in a previous study; [30] (ii) vehicle-treated mice, with normal saline treatment; (iii) control mice; and (iv) ribavirin-treated mice. The mice were lightly anesthetized with diethyl ether and then infected intranasally with 10^6 plaque-forming units of RSV diluted in PBS in a total volume of 50 μL [31, 32]. An equal volume of PBS served as the mock infection. To determine whether probiotics could exhibit therapeutic potential, the probiotics were administered orally on a daily basis starting from either 1 week in advance (PP) or on the same day (PT) of RSV infection. The vehicle-treated groups received normal saline. The doses of *LGG*, *ECN*, and *VSL#3* were 10^8 CFU per mouse in one day. Ribavirin-treated mice received 46 $mg \cdot kg^{-1} \cdot d^{-1}$. All mice were sacrificed by cervical dislocation at day 3. The mouse lung tissue was removed and weighed. The lung index was calculated by the following formula: lung index=lung weight/body weight.

Gut microbiota depletion

The mice were gavaged daily for 10 days with an antibiotic cocktail (ABX) containing 0.35 mg/mL gentamycin (Fresenius Kabi, China), 5.25 mg/mL kanamycin (JINYIBAI, China), 8500 U colistin (JINYIBAI, China), 2.15 mg/mL metronidazole (JINYIBAI, China), and 0.5 mg/mL vancomycin (Sigma-Aldrich, USA) [33].

Histologic and immunohistochemical analyses

Sections (4 μm) were cut from paraffin-embedded lung tissue, fixed in formalin (Beyotime, Shanghai, China), and stained with hematoxylin and eosin.

Albumin analyses

BALF was collected, and the total albumin protein was determined using the Mouse Albumin ELISA Quantitation Set according to the manufacturer's instructions. BALF was applied at dilutions of 1:100.

Flow cytometry assay

Protocols of intracellular staining for measuring IRF3 and TBK1 phosphorylation were used. For fixation, cells were pelleted by centrifugation and the supernatant was removed. Then, the cells were resuspended in ~100 μL of 4% formaldehyde per 1 million cells. The pellets were mixed well to dissociate and prevent the

cross-linking of individual cells and then fixed for 15 min at room temperature (20–25 °C), followed by washing by centrifugation with excess 1× PBS. The supernatant was discarded in an appropriate waste container. The cells were resuspended in 0.5–1 mL 1× PBS. For the permeabilization step, ice-cold 100% methanol was slowly added to the prechilled cells while gently vortexing to a final concentration of 90% methanol. The cells were permeabilized for a minimum of 10 min on ice.

For phosphor-IRF3-PE immunostaining, the cells were washed by centrifugation in excess 1× PBS to remove methanol. The supernatant was discarded in the appropriate waste container. The cells were resuspended in 100 µL of diluted P-IRF3-PE, prepared in antibody dilution buffer at a recommended dilution of 1:50, incubated for 1 h at room temperature, protected from light, and washed by centrifugation in 1× PBS. The supernatant was discarded, and the cells were resuspended in 200 µL of 1× PBS and analyzed by flow cytometry.

For phosphor-TBK1 immunostaining, the cells were washed by centrifugation in excess 1× PBS to remove methanol. The supernatant was discarded in the appropriate waste container. The cells were resuspended in 100 µL of diluted P-TBK1, prepared in antibody dilution buffer at a recommended dilution of 1:50, incubated for 1 h at room temperature, and washed by centrifugation in 1× PBS. The supernatant was discarded, and the cells were resuspended in 100 µL of diluted Alexa Fluor 647-conjugated goat anti-rabbit IgG secondary antibody and incubated for 30 min at room temperature in the dark. This step was followed by washing by centrifugation in 1× PBS. The supernatant was discarded, and the cells were resuspended in 200 µL of 1× PBS and analyzed by flow cytometry. Annexin V-FITC and PI Apoptosis kits were used to examine the mortality of AMs in vivo. All of the flow cytometry data were acquired with a BD Accuri C6 Plus flow cytometer and analyzed by FlowJo software.

Immunofluorescence analyses

For staining lung tissues, thin sections (4 µm) were blocked with 1% bovine serum albumin and then incubated with primary antibodies and RSV-F protein antibody overnight at 4 °C. After three times washing with PBS, the sections on slides were incubated with fluorescence-conjugated secondary antibodies at room temperature for 2 h. Sections incubated with secondary antibodies alone were used as negative controls. Finally, DAPI was used to stain the nuclei of cells. Images were taken at random fields under a microscope.

RNA extraction and quantitative real-time PCR

Total RNA was isolated using TRIzol Reagent (Invitrogen) according to the manufacturer's instructions. Real-time PCR assays were then performed using SYBR green dye (Bio-Rad) on a Step One Sequence Detection System (Applied Biosystems, Waltham, MA, USA). The relative abundance of genes was calculated by using the $2^{-\Delta\Delta CT}$ formula, with GAPDH as an internal control. The primer sets used are detailed in Supplementary Table S1.

Alveolar macrophage isolation and depletion

AMs were obtained from BALB/c mice as previously described [34]. AMs were cultured in RPMI-1640 medium (Gibco, Grand Island, NY, USA) supplemented with 10% FBS (Gibco) at 37 °C in a humidified atmosphere with 5% CO_2. For the depletion of macrophages, the mice were inoculated intranasally with a single dose of 100 µL of L-CL^{2}MBP as described elsewhere [35]. Equal volumes of PBS served as controls [31].

Enzyme-linked immunosorbent assay (ELISA)

Lungs were homogenized in a buffer solution (1 mL/0.1 g). Then, supernatants were collected to detect the expression of IFNβ. Broncho-alveolar lavage fluid (BALF) and serum were also collected to detect the levels of IFNβ and SCFAs. Cytokine analysis was performed using a mouse IFNβ ELISA kit (R&D Systems Minneapolis, MN, USA). Absorbance was determined using an ELx-800 Universal Microplate Reader (BIO-TEK, Vermont, USA).

DNA extraction and PCR amplification

Microbial DNA was extracted from feces and BALF using the E.Z.N. A.® Soil DNA Kit (Omega Bio-Tek, Norcross, GA, USA) according to the manufacturer's protocols. The V4-V5 region of the bacterial 16 S ribosomal RNA gene was amplified by PCR (95 °C for 2 min, followed by 25 cycles at 95 °C for 30 s, 55 °C for 30 s, and 72 °C for 30 s and a final extension at 72 °C for 5 min) using the primers 515 F 5′-barcode-GTGCCAGCMGCCGCGG-3′ and 907 R 5′-CCGTCAATT CMTTTRAGTTT-3′, where the barcode is an eight-base sequence unique to each sample. PCRs were performed in triplicate in a 20 µL mixture containing 4 µL of 5× FastPfu Buffer, 2 µL of 2.5 mM dNTPs, 0.8 µL of each primer (5 µM), 0.4 µL of FastPfu Polymerase, and 10 ng of template DNA. Amplicons were extracted from 2% agarose gels, purified using the AxyPrep DNA Gel Extraction Kit (Axygen Biosciences, Union City, CA, USA) according to the manufacturer's instructions and quantified using QuantiFluor-ST (Promega, USA).

Library construction and sequencing

Purified PCR products were quantified by a Qubit® 3.0 fluorometer (Life Technologies Corporation), and every twenty-four amplicons whose barcodes were different were mixed equally. The pooled DNA product was used to construct the Illumina Pair-End library following Illumina's genomic DNA library preparation procedure. Then, the amplicon library was paired-end sequenced (2×250) on an Illumina MiSeq platform (Shanghai BIOZERON Co., Ltd.) according to standard protocols.

Processing of sequencing data

Raw FASTQ files were demultiplexed and quality-filtered using QIIME (version 1.17) with the following criteria. (i) The 250 bp reads were truncated at any site, receiving an average quality score of <20 over a 10 bp sliding window, discarding the truncated reads that were shorter than 50 bp. (ii) Reads had exact barcode matching, with 2 nucleotide mismatches in primer matching, and reads containing ambiguous characters were removed. (iii) Only sequences that overlapped longer than 10 bp were assembled according to their overlap sequence. Reads that could not be assembled were discarded.

Operational taxonomic units were clustered with a 97% similarity cutoff using UPARSE (version 7.1, http://drive5.com/uparse/), and chimeric sequences were identified and removed using UCHIME. The phylogenetic affiliation of each 16 S rRNA gene sequence was analyzed by RDP Classifier (http://rdp.cme.msu.edu/) against the Silva (SSU123) 16 S rRNA database using a confidence threshold of 70% [36].

Analysis of α and β diversity

The rarefaction analysis based on Mothur v.1.21.1 [37] was conducted to reveal the diversity indices, including the Chao, ACE, and Shannon diversity indices. The β diversity analysis was performed using UniFrac to compare the results of principal component analysis (PCA) using the community ecology package R-forge (the Vegan 2.0 package was used to generate a PCA figure). To examine the dissimilarities in community composition, we performed PCoA in QIIME. PCoA, where a distance matrix is used to plot n samples in an $(n-1)$-dimensional space, was used to compare groups of samples based on unweighted and weighted UniFrac distance metrics.

Metabolite extraction

For metabolite extraction, 700 µL of sample was placed into 2 mL EP tubes, with 350 µL of methanol used as the extraction liquid and 10 µL of adonitol (0.5 mg/mL stock in ddH_2O) used as the internal

standard. This mixture was vortexed for 30 s, kept at −20 °C for 10 min, and then ultrasound treated for 10 min (incubated in ice water). This step was followed by centrifugation for 15 min at 12000 r/min and 4 °C. Then, 1000 μL of supernatant was transferred into a fresh 1.5 mL EP tube and dried completely in a vacuum concentrator without heating. After incubation with 20 μL of methoxyamination hydrochloride (20 mg/mL in pyridine) for 30 min at 80 °C, 30 μL of the BSTFA reagent (1% TMCS, *v/v*) was added to the sample aliquots and incubated for 1.5 h at 70 °C. All samples were analyzed by a gas chromatograph system coupled with a Pegasus HT time-of-flight mass spectrometer (GC-TOF-MS).

GC-TOF-MS analysis

GC-TOF-MS analysis was performed using an Agilent 7890 gas chromatograph system coupled with a Pegasus HT time-of-flight mass spectrometer. The system utilized a DB-5MS capillary column coated with 5% diphenyl cross-linked with 95% dimethylpolysiloxane (30 m × 250 μm inner diameter, 0.25 μm film thickness; J&W Scientific, Folsom, CA, USA). A 1 μL aliquot of the analyte was injected in splitless mode. Helium was used as the carrier gas, the front inlet purge flow was 3 mL/min, and the gas flow rate through the column was 1 mL/min. The initial temperature was kept at 50 °C for 1 min, raised to 310 °C at a rate of 20 °C/min, and then kept for 6 min at 310 °C. The injection, transfer line, and ion source temperatures were 280 °C, 280 °C, and 250 °C, respectively. The energy was -70 eV in electron impact mode. The mass spectrometry data were acquired in full-scan mode with an *m/z* range of 50–500 at a rate of 12.5 spectra per second after a solvent delay of 6.13 min.

Data preprocessing and annotation

Chroma TOF 4.3× software from LECO Corporation and LECO-Fiehn Rtx5 database were used for raw peak exacting, data baseline filtering and calibration of the baseline, peak alignment, deconvolution analysis, peak identification, and integration of the peak area. Both mass spectrum matches and retention index matches were considered in metabolite identification.

Statistical analysis

All of the data, unless otherwise indicated, are presented as the means ± SDs of three independent experiments. The statistical significance of the differences between two groups was analyzed with Student's *t* test. Multiple group comparisons were performed by one-way ANOVA followed by Bonferroni post hoc *t* test. All of the calculations were performed using the Prism software program for Windows (GraphPad Software). A *P* value of 0.05 or less was considered statistically significant.

RESULTS

Probiotic mixture intake protects against RSV-induced lung pathology and displays anti-RSV infection properties

To determine whether the probiotics exhibit therapeutic potential in RSV infection, the probiotics were administered orally on a daily basis starting from either 1 week in advance (PP) or on the same day (PT) of RSV infection (Fig. 1a), and ribavirin was used as a positive drug. Histological analyses of lung tissues in RSV-infected mice showed that both PP and PT treatment improved lung inflammation compared with vehicle and ribavirin treatment (Figs. 1b, c). As shown in Fig. 1d, the lung index (lung weight/body weight) was also improved in the PP and PT groups compared to the vehicle group. The albumin infiltrate in bronchoalveolar lavage fluid (BALF) was also reduced in the PP group compared to the vehicle group (Fig. 1e), indicating the protective effects of probiotics on lung injury. In addition, treatment with the probiotics (PP and PT) prevented weight loss (Supplementary Fig. S1a). Collectively, these data suggested that PP and PT treatment had positive effects on lung immunopathology in RSV-infected mice.

The expression of pro-inflammatory cytokines, such as IL-1β and IL-6, was examined in the lung. Both PP and PT treatment reduced the expression of these cytokines in RSV-infected mice (Supplementary Fig. S1b and S1c). PT and PP treatment also significantly decreased lymphocyte infiltration, represented by reduced percentages of $CD4^+$ T cells and monocytes in BALF (Supplementary Fig. S1d and S1e). These data indicate that the probiotics exert significant protective effects against RSV-induced lung inflammation. These data are consistent with the results of a previous study showing that this probiotic mixture possessed anti-inflammatory efficacy [30].

To investigate whether the probiotic mixture defends against RSV infection, the viral load in the lungs was examined three days after RSV infection using qPCR and immunofluorescence assays. We observed that PP significantly reduced the viral load in lung tissue, as shown by decreased expression of RSV fusion protein (Fig. 1f) and viral protein F expression in the lungs of RSV-infected mice (Figs. 1g, h). Surprisingly, PT treatment did not exert efficacy in RSV load reduction in the lungs. These results suggested that the intake of the preventive probiotic mixture exerted antiviral effects against RSV infection. We next explored the anti-RSV mechanism of PP treatment and why PP treatment exerted anti-RSV effects, while PT treatment did not.

The preventive probiotic mixture reverses RSV-induced gut dysbiosis

Given that gut dysbiosis was found in RSV-infected mice [2], we examined the effects of the probiotic mixture on gut dysbiosis in RSV-infected mice. We first noted that the α-diversity, the representative parameter of richness and diversity of gut microbiota, as calculated by the Shannon index, was significantly decreased in RSV-infected mice compared to their healthy control littermates (Fig. 2a). The decreased Shannon α-diversity was reversed by PP treatment, while PT treatment failed to influence Shannon α-diversity in RSV-infected mice (Fig. 2a). Principal coordinate analysis revealed a distinct shift in gut microbial composition in RSV-infected mice compared with healthy controls (Fig. 2b). Both PT and PP treatment significantly shortened the intergroup difference of gut microbiota induced by RSV infection, while PP treatment exerted greater efficacy than PT (Fig. 2b).

A previous study showed that RSV infection resulted in significantly altered gut microbiota composition, with an increase in *Bacteroidetes* and a decrease in *Firmicutes* abundance [2], and we also observed this phenomenon (Figs. 2c-e). PP treatment significantly improved the changed composition of the gut microbiota, such as *Firmicutes* and *Bacteroides*, at the phylum level in RSV-infected mice (Figs. 2c-e). PP treatment also restored other dominant bacteria (>1% in any sample), such as *Proteobacteria* and *Actinobacteria* (Supplementary Fig. S2a and S2b), at the phylum level.

We further conducted a detailed analysis of the gut microbiota at the genus level after probiotic mixture treatment in RSV-infected mice. PP treatment significantly restored the levels of dominant bacteria, such as *Lachnospiraceae NK4A136* group, *Bacteroidales S24-7* group_norank (Fig. 2f-h), *Lachnospiraceae*_uncultured, and *Ruminiclostridium* (Supplementary Fig. S2c and S2d). At the species level, PP significantly restored the levels of dominant bacteria, such as *Lachnospiraceae*_uncultured bacterium and *Lachnospiraceae NK4A136* group_uncultured bacterium (Fig. 2i, and Supplementary Fig. S2e). Overall, this result showed that the intake of the preventive probiotic mixture could reverse RSV-induced gut dysbiosis by modulating the diversity and composition of the gut microbiota.

The preventive probiotic mixture increases the abundance of SCFA-producing bacteria and the levels of SCFAs in RSV-infected mice

A previous study showed that *Firmicutes* constituted the majority of SCFA producers [38]. RSV infection induced a decreased

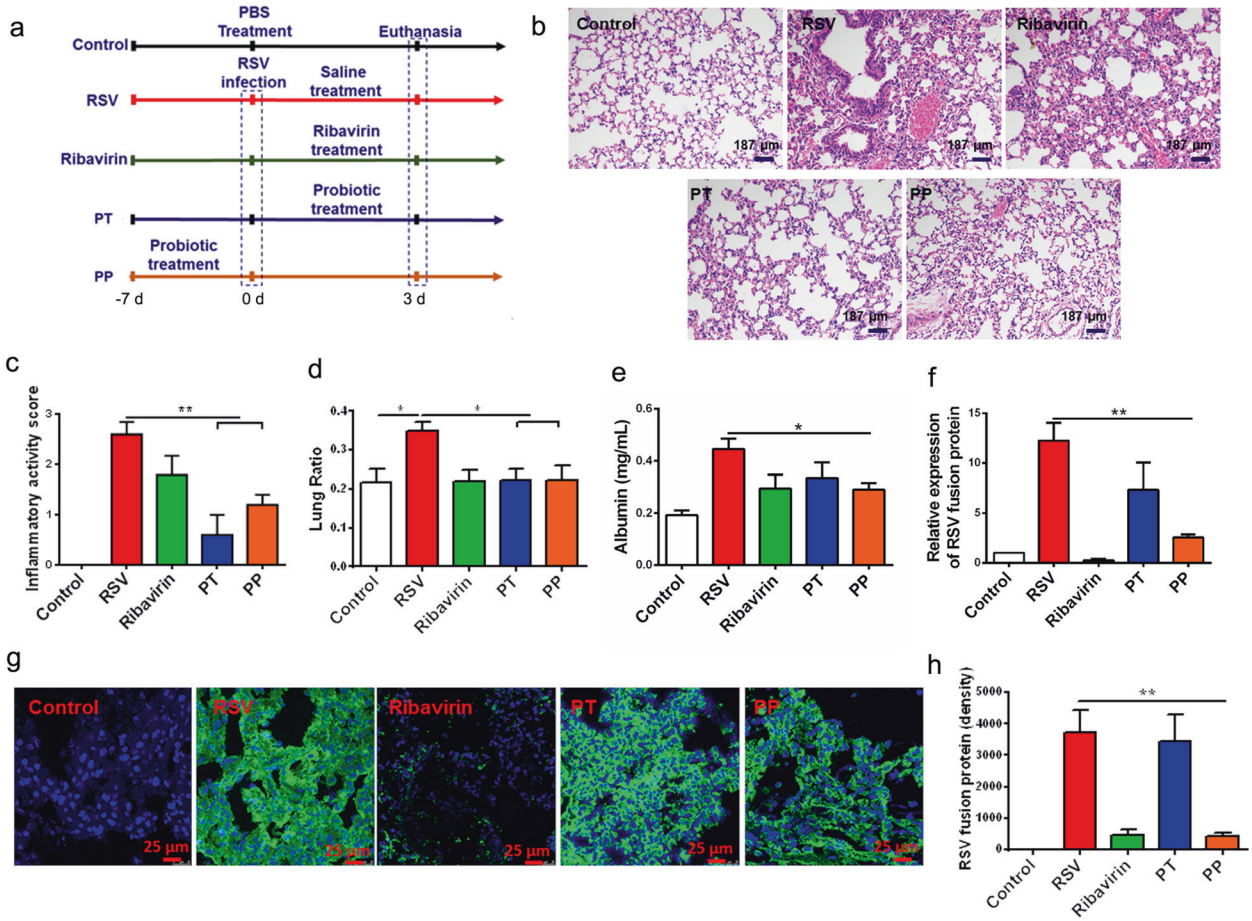

Fig. 1 Probiotics showed an antiviral response to RSV infection. a The experimental design. **b**, **c** Representative H&E-stained lung tissue from mice showed histologic differences (n=5). **d** The lung index was measured and presented as a percentage of lung weight/body weight (n=8). **e** The albumin level in BALF was determined (n=5). **f** The viral load in the lungs of mice was measured by viral RNA expression in relation to GAPDH (n=4). **g**, **h** RSV-F protein staining for evaluating the viral load in the lungs of mice using immunofluorescence (n=4). Green: RSV-F protein; Blue: DAPI. All results are expressed as the mean±SD (**b**–**g**). $^{*}P<0.05$, $^{**}P<0.01$ by Student's t test.

abundance of *Firmicutes*, while PP treatment significantly reversed the levels of *Firmicutes* (Fig. 2e). This finding might be indicative of the increased production of SCFAs in PP-treated mice. Moreover, at the genus level, SCFA-producing bacteria, such as *Lachnospiraceae NK4A136* group, *Lachnospiraceae*_uncultured, and *Clostridiales vadinBB60* group_norank, were reduced in RSV-infected mice, while PP treatment also significantly recovered these bacteria (Figs. 2g, 3a, b). Furthermore, at the species level, PP treatment also increased SCFA-producing bacteria in RSV-infected mice, such as *Lachnospiraceae*_uncultured bacterium, *Lachnospiraceae NK4A136* group_uncultured bacterium (Fig. 2i, j), and *Blautia*_uncultured bacterium (Fig. 3c). The increased ratio of SCFA-producing bacteria indicated that the production of SCFAs might be elevated in PP-treated mice.

To support this hypothesis, gas chromatography-mass spectrometry was utilized to quantify SCFA levels, and our data showed that PP treatment restored the concentrations of acetate, propionate, and butyrate in feces (Fig. 3d-f). It is known that SCFAs produced in the gut can pass into the systemic circulation and then exert remote biological effects (particularly acetate and, to a lesser extent, propionate and butyrate) [4]. In our study, PP treatment also increased SCFA serum levels (Fig. 3j-l). Altogether, our results revealed that the preventive probiotic mixture can increase SCFA-producing bacteria and elevate the levels of SCFAs in RSV-infected mice.

The preventive probiotic mixture restores RSV-induced lung microbiota alteration

The airway microbiota has been found to be substantially altered in the context of numerous respiratory disorders [39], while whether RSV infection influences the lung microbiota is unknown. In this study, BALF from RSV-infected mice was collected, and 16 S RNA sequencing was performed to investigate the lung microbiota. As shown in Fig. 4a, the Shannon α-diversity was significantly decreased in RSV-infected mice, while PP treatment markedly increased Shannon α-diversity. Principal coordinate analysis revealed that the lung microbial composition in RSV-infected mice was distinct from that in control mice, while PP treatment led to a significant improvement in the alteration of lung microbial composition (Fig. 4b).

We next analyzed the composition of the dominant lung microbiota at three different taxonomic levels. At the phylum level, dominant bacteria, such as *Bacteroidetes* and *Actinobacteria*, were significantly reduced, while the ratio of these bacteria was reversed in PP group mice (Fig. 4c, d). At the genus level, our results showed that PP treatment dramatically restored the dominant bacteria, including *Caulobacteraceae*_Unclassified, *Mesorhizobium*, *Bradyrhizobium*, and *Algibacter* (Fig. 4e-h). At the species level, PP treatment dramatically restored the dominant bacteria, including *Sphingomonas paucimobilis*, *Caulobacteraceae_Unclassified*, *Altererythrobacter*_Unclassified (Fig. 4i-k), *Bradyrhizobium*_Unclassified, and

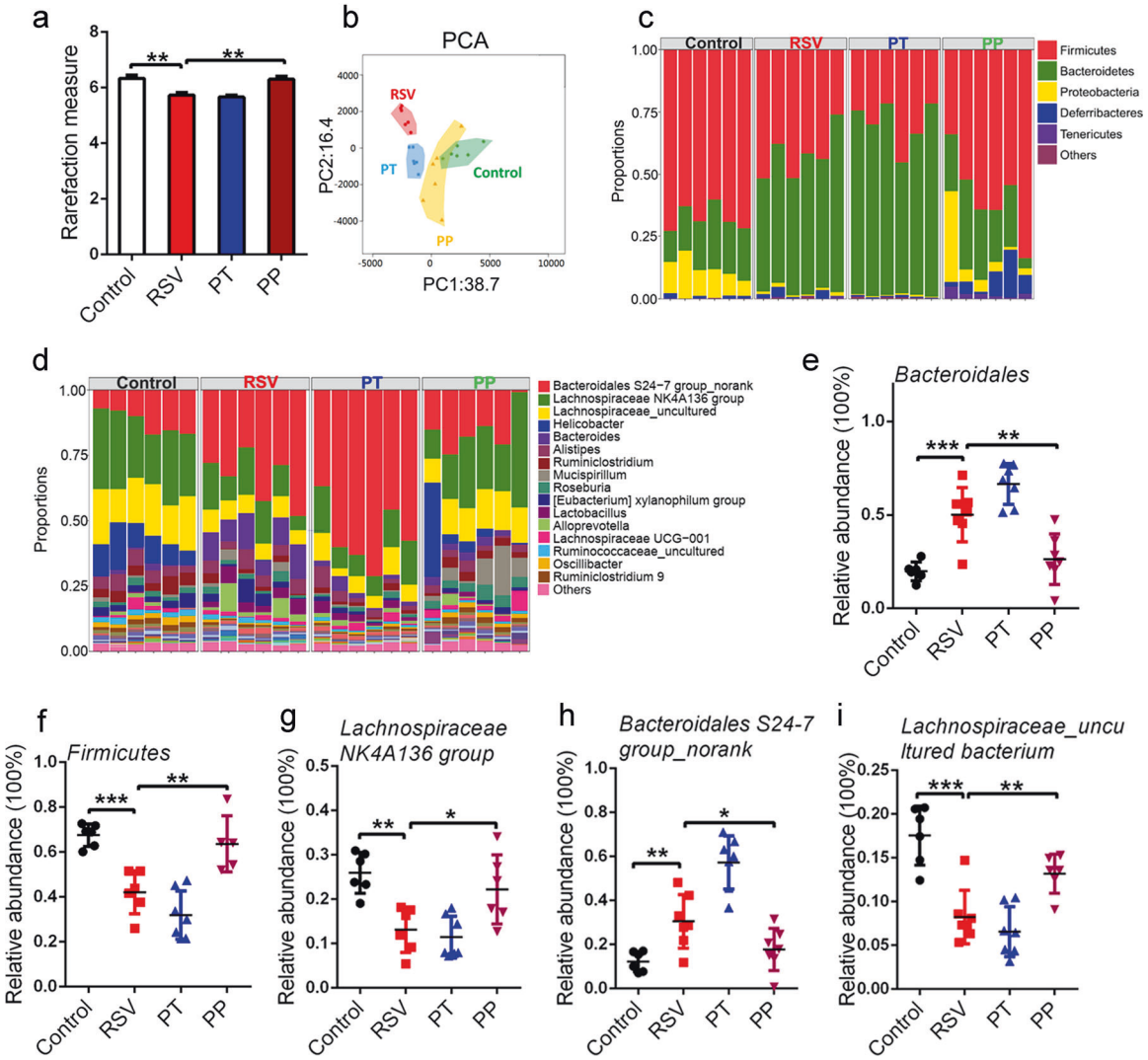

Fig. 2 Probiotics reversed gut dysbiosis. a Gut microbial Shannon diversity was analyzed in all groups of mice (n=5). **b** Principal coordinate analysis of the gut microbiota of mice was conducted in all groups of mice (n=6). **c**–**e** The relative abundance of the dominant gut microbiota (>1% in any sample) at the phylum level was measured (n=6 or 7). **f**–**h** The relative abundance of the dominant bacteria (>1% in any sample) at the genus level was examined (n=6 or 7). **i** The relative abundance of the dominant bacteria (>1% in any sample) at the species level was examined (n=6 or 7). All results are expressed as the mean±SD (**a**–**j**). *P<0.05, **P<0.01, ***P<0.001 by Student's t test.

*Algibacter*_Unclassified (Supplementary Fig. S3a, S3b). Taken together, these results indicated that the structure and diversity of the lung microbiota was substantially altered in RSV-infected mice, and the preventive probiotic mixture could reverse RSV-induced lung microbiota disorders by modulating the diversity and composition of the lung microbiota.

A previous study indicated that gut microbiota significantly influenced lung microbiota composition [40], and dietary fermentable fiber changed the composition of lung microbiota, in particular by decreasing the *Firmicutes* to *Bacteroidetes* ratio [41], indicating that gut microbiota-derived SCFAs might influence lung microbiota. Thus, we evaluated the *Firmicutes* to *Bacteroidetes* ratio in RSV-infected mice after PP treatment and found that the *Firmicutes* to *Bacteroidetes* ratio was decreased, which was consistent with the finding of a previous study [41]. However, PP treatment decreased the *Firmicutes* to *Bacteroidetes* ratio in RSV-infected mice (Fig. 4l), indicating that the modulation of the lung microbiota of the probiotic mixture might occur through SCFAs.

The preventive probiotic mixture may potentially modulate alveolar macrophages (AMs) via lung microbiota

The lung microbiota had previously been shown to interact with the immune system, modulating immune responses [17, 19]. To characterize the potential relationship between lung microbiota and lung immunity, we performed PICRUSt analysis combined with the Kyoto Encyclopedia of Genes and Genomes database of microbial genomic information. This analysis revealed that PP treatment influenced Fcγ receptor-mediated phagocytosis and endocytosis (Fig. 5a). Alveolar macrophages (AMs) constitute the main lung phagocytes and perform phagocytosis via the Fcγ receptor [42]. Therefore, we speculated that PP treatment might influence AMs via lung microbiota.

A recent study demonstrated that in infant mice, intranasal administration of *Corynebacterium pseudodiphtheriticum*, which was present in the respiratory tract, was able to reduce the features of RSV infection through the regulation of AMs [23]. *Corynebacterium* can not only increase the percentages of AMs but also promote AM secretion of IFN-β by activating the TLR3 signaling pathway [23].

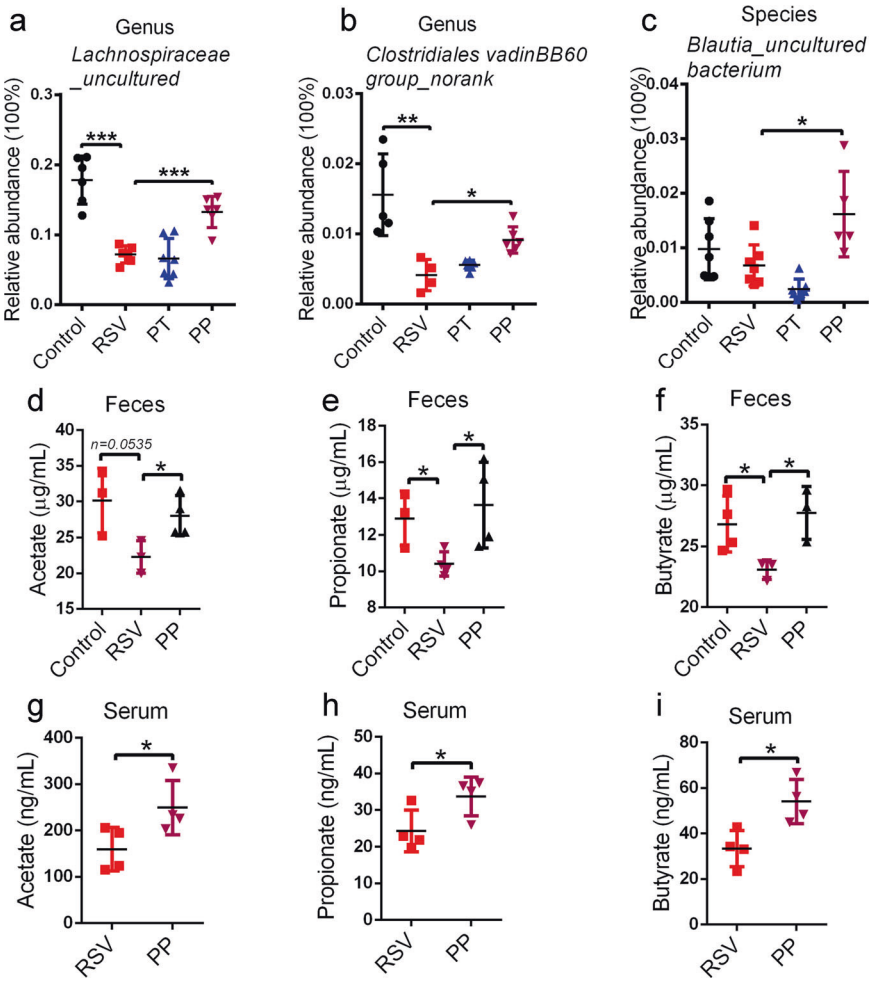

Fig. 3 Probiotics increased the levels of SCFAs. a, **b** The relative abundance of fecal SCFA-producing bacteria at the genus level was examined (n=6 or 7). **c** The relative abundance of fecal SCFA-producing bacteria at the species level was examined (n=5 or 6). **d**–**f** The fecal levels of SCFAs in mice were measured by GC-MS (n=3 or 4). **g**–**i** The serum levels of SCFAs in mice were measured by GC-MS (n=4). All results are expressed as the mean±SD (**a**–**i**). *P<0.05, **P<0.01, ***P<0.001 by Student's t test.

A previous study reported that *Lactobacillus* also exerted an antiviral immune response by promoting the macrophage secretion of IFN-β [43]. These studies suggested that modulating lung immune responses by lung microbiota might partly occur through *Corynebacterium* and *Lactobacillus*. As such, we measured the levels of *Corynebacterium* and *Lactobacillus* in the lung microbiota of RSV-infected mice after probiotic mixture treatment. As shown in Fig. 5b and c, the abundance of *Corynebacterium* at the genus and species levels was significantly increased in the lungs after PP treatment. Our data showed that PP treatment did not influence *Lactobacillus* at the genus level (Fig. 5d) but markedly elevated the species levels of *Lactobacillus gallinarum* and *Lactobacillus*_uncultured bacterium (Fig. 5e, f) in the lungs of RSV-infected mice. Collectively, our results showed that the preventive probiotic mixture might potentially modulate AMs to influence lung immunity via lung microbiota. How the intake of preventive probiotics influences lung microbiota has been of interest, with some previous studies demonstrating that SCFAs are important carbon sources for *Corynebacterium* and *Lactobacillus* reproduction [44–46], thus suggesting that the increase in *Corynebacterium* and *Lactobacillus* in probiotic mixture-treated mice may be attributed to SCFAs.

The preventive probiotic mixture promotes AM secretion of IFN-β

AMs are the first line of cellular defense against respiratory viral infection through the secretion of type I IFNs [47, 48]. The depletion of AMs by either genetic knockout or clodronate treatment increases morbidity, mortality, and viral load during RSV infection [31]. Our results indicated that the preventive probiotic mixture might regulate AMs via *Corynebacterium* and *Lactobacillus* in the lungs and that *Corynebacterium* and *Lactobacillus* could promote IFN-β secretion in macrophages. Moreover, acetate has been shown to directly influence the function of AMs [4] and induce IFN-β production in A549 cells [13]. These studies suggest that the probiotic mixture can influence AMs through lung microbiota (*Corynebacterium* and *Lactobacillus*) and acetate.

We investigated this hypothesis in vitro by assessing IFN-β expression in freshly isolated AMs exposed to acetate (270 μM) for 2 h prior to infection with RSV for 2, 6, and 12 h. qPCR analysis revealed that acetate treatment significantly increased IFN-β expression (Fig. 6a). Furthermore, AMs were isolated from BALF, as previously described [34], and we found that PP treatment significantly elevated IFN-β expression in AMs in a time-dependent manner following RSV infection (Fig. 6b). The evaluation of IFN-β in the lungs and serum after the probiotic mixture treatment showed that its mRNA and protein levels significantly increased in PP-treated mice following RSV infection (Fig. 6c and d). Thus, these results suggest that the probiotic mixture provides protection against RSV infection by modulating AM-derived IFN-β production.

To further demonstrate this point, IFNAR1 was blocked using a neutralizing antibody in RSV-infected mice [49], resulting in the

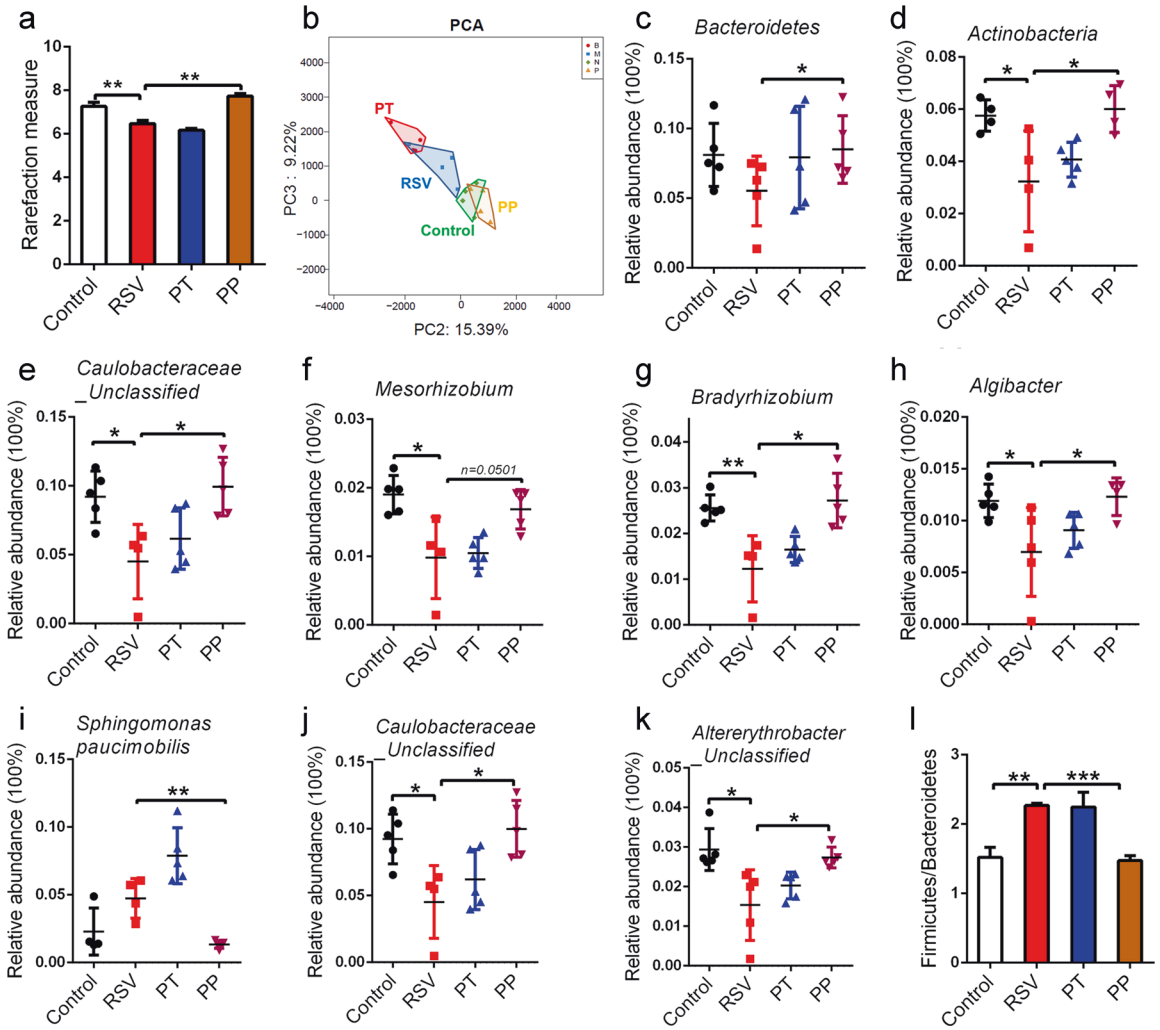

Fig. 4 Probiotics restored RSV-induced lung microbiota alteration. a Lung microbial Shannon diversity analysis was performed (n=4). **b** Principal coordinate analysis of the lung microbiota of mice was conducted (n=4). **c**, **d** The relative abundance of the dominant lung microbiota (>1% in any sample) at the phylum level was measured (n=4 or 5). **e**–**h** The relative abundance of the dominant bacteria at the genus level was examined (n=4 or 5). **i**–**k** The relative abundance of the dominant bacteria at the species level was examined (n=4 or 5). (**l**) Representation of the Firmicutes/Bacteroidetes ratios at the phylum level (n=4). All results are expressed as the mean±SD (**a**–**l**). *P<0.05, **P<0.01, ***P<0.001 by Student's t test.

loss of the antiviral protective effects of the probiotic mixture on RSV-infected mice (Fig. 6e). These data confirmed that the probiotic mixture defended against RSV infection by elevating IFN-β levels in RSV-infected mice.

To confirm the roles of AMs in the anti-RSV effects of the probiotic mixture, AMs were depleted from the lungs via intranasal administration of 100 μL of clodronate liposomes, according to a previous study [4, 31]. AM deletion attenuated the anti-RSV effects of the probiotics (Fig. 6f). Collectively, our results showed that the preventive probiotic mixture exerts anti-RSV effects mainly through AM-derived IFN-β.

Previous studies showed that RSV infection activated IRF3 via TBK1- and IKKi-dependent phosphorylation [50], leading to the production of IFN-β in AMs [51]. Thus, we examined the status of the TBK1-IRF3 pathway in AMs after PP treatment using flow cytometry after intracellular staining. PP treatment significantly increased the serine phosphorylation (Ser172) of TBK1 and the serine phosphorylation (Ser396) of IRF3 in AMs 24 h postinfection (Fig. 6g, h), implying that the preventive probiotic mixture promoted IFN-β production in AMs by activating the TBK1/IRF3 pathway.

The antiviral effects of the probiotic mixture are mediated by gut microbiota-derived acetate

To explore the roles of gut microbiota and acetate in the therapeutic effects of the probiotic mixture, ABX and acetate supplement experiments were utilized (Fig. 7a). The ABX cocktail is commonly used to disrupt gut microbiota [33]. Prior to treatment with the probiotic mixture, the mice were gavaged daily with ABX for 10 days. Afterwards, the mice were preventively treated with the probiotic mixture for 7 days. Moreover, the mice in the ABX-probiotic-ACE group were additionally supplemented with 200 mM acetate in their drinking water. The results revealed that the protective effects of the probiotic mixture were attenuated in ABX-treated mice, represented by the augmented RSV load (Fig. 7b and Supplementary Fig. S4a). In contrast, acetate supplementation restored the therapeutic effects of the probiotic mixture on RSV infection (Fig. 7b). The probiotic mixture failed to increase IFN-β expression in the AMs of ABX-treated mice, while acetate supplementation restored IFN-β expression in AMs (Fig. 7c). Acetate supplementation also restored IFN-β levels in the BALF of ABX-treated mice (Fig. 7d). As expected, acetate supplementation significantly impeded disease progression and

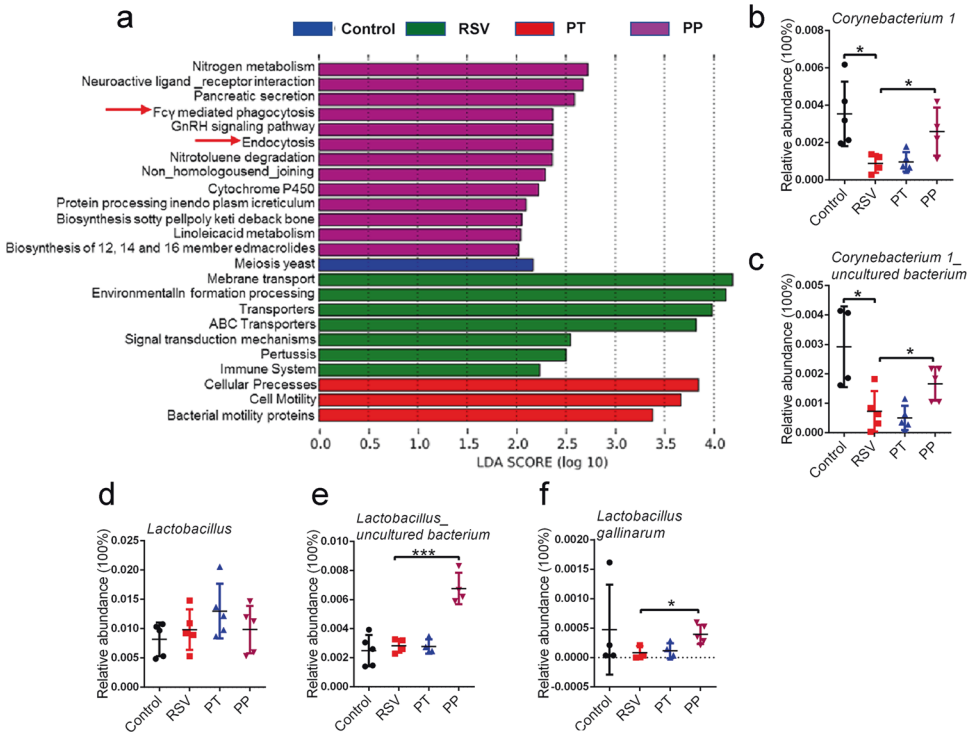

Fig. 5 Probiotics may potentially activate the antiviral responses of alveolar macrophages. a PICRUSt analysis combined with the Kyoto Encyclopedia of Genes and Genomes (KEGG) database of microbial genomic information. **b**, **c** The relative abundance of *Corynebacterium* at the genus and species levels was examined (n=4 or 5). **d**–**f** The relative abundance of *Lactobacillus* at the genus and species levels was examined (n=4 or 5). All results are expressed as the mean±SD (**b**–**f**). *P<0.05, ***P<0.001 by Student's t test.

reduced lung inflammation and inflammatory scores (Fig. 7e and Supplementary Fig. S4a), improving lung injury (Fig. 7f). Therefore, these findings support that the probiotic mixture defense against RSV infection occurred via a gut microbiota-acetate-AM axis.

Next, we conducted microbiota transfer studies using a cohousing experiment. It is believed that gut microbiota can be transmitted horizontally between mice in the same cage, owing to their coprophagic behavior [52]. Mice that underwent 1-week pretreatment with probiotics were either housed singly or cohoused with PBS-treated mice for an additional week and then challenged with RSV (Supplementary Fig. S4b). IFN-β levels in AMs were elevated in CoHo-PBS mice compared to mice treated with PBS exclusively (Supplementary Fig. S4c). These data suggested that the promotion of the AM secretion of IFNβ by the probiotic mixture is transmissible through cohousing microbiota transplantation, and these data confirmed the involvement of the gut microbiome in the anti-RSV effects of the probiotic mixture.

DISCUSSION

In the current study, the probiotic mixture restored the RSV-induced dysbiosis in the gut and increased the levels of SCFA-producing microbiota, which consequently led to elevated levels of SCFAs. The probiotic mixture markedly reduced lung RSV replication by modulating the innate antiviral response, and the antiviral immunity responses in mice fed the probiotic mixture were mediated by AM-derived IFN-β. Our results showed that probiotic mixture treatment induced IFN-β production in AMs via acetate. Moreover, we found that the probiotic mixture restored the RSV-induced lung microbiota dysbiosis, and functional prediction indicated that the probiotic mixture might potentially regulate AMs via the lung microbiota. Further experiments showed increased levels of *Corynebacterium* and *Lactobacillus* in the lungs, which could promote the AM production of IFN-β, in probiotic mixture-treated mice. Based on a previous study, we speculate that the modulation of lung microbiota by the probiotic mixture may occur through SCFAs. Overall, our study indicated that the probiotic mixture protected against RSV infection by modulating the microbiota-AM axis.

Our study revealed that the probiotic mixture was effective in defending against RSV infection; gut and lung dysbiosis were restored when the probiotic mixture was administered 1 week in advance of RSV infection. The probiotic mixture administered the same day of RSV infection exerted significant protective effects against RSV-induced lung inflammation but failed to display efficacy in reversing gut and lung dysbiosis. The anti-inflammatory effects of the probiotic mixture administered on the same day of RSV infection were consistent with those reported in previous studies [30]. Early intake of the probiotic mixture may change the structure and composition of the gut microbiota, for example, by increasing the levels of SCFA-producing bacteria, which leads to elevated levels of SCFAs. SCFAs have been well documented for their anti-inflammatory and antiviral effects. Thus, we believe that the therapeutic effect of the early intake of the probiotic mixture may occur through the modulation of gut microbiota.

Consistent with that in a previous study, RSV induced a significant increase in the relative abundance of *Bacteroidetes* and a decrease in *Firmicutes* at the phylum level [2], while the probiotic mixture significantly restored these bacteria, suggesting that this mixture was effective in mediating gut dysbiosis in RSV infection. Further results indicated that the probiotic mixture reversed RSV-induced gut dysbiosis by modulating the diversity and composition of the gut microbiota. A previous study indicated that the levels of SCFA-producing bacteria were downregulated in RSV-infected mice [2], and probiotic intake drastically increased the metabolic potential of SCFA production. In our results, the probiotic mixture significantly increased the levels of SCFA-producing bacteria, such as *Firmicutes* at the phylum level, *Lachnospiraceae NK4A136* at the genus level, and *Lachnospiraceae*_uncultured bacterium at the species level. Further experiments confirmed that the probiotics increased the

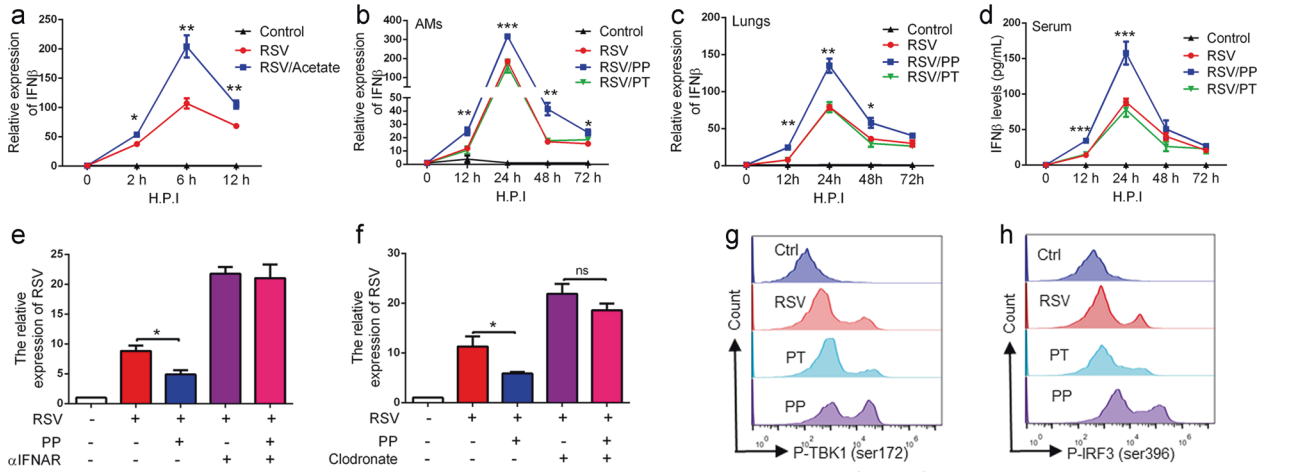

Fig. 6 Probiotic pretreatment promoted IFN-β production in AMs. a Isolated AMs were pretreated with acetate and then stimulated with RSV (1 MOI) at the indicated time points. The levels of IFN-β were tested by qPCR. The results are from three independent experiments. **b** Quantification of IFN-β in sorted AMs from all groups of mice by qPCR (n=4). **c** Quantification of IFN-β in lungs from all groups of mice by qPCR (n=4). **d** Levels of IFNβ in serum from all groups of mice were examined by ELISA (n=4). **e** IFNAR1 was blocked using a neutralizing antibody in RSV-infected mice, and we then evaluated the effects of the probiotics on RSV infection. RSV mRNA expression in the lungs was examined using qPCR at 3 days after RSV infection (n=4). αIFNAR, antibody against IFNAR. **f** For the depletion of macrophages, the mice were intranasally inoculated with a single dose of 100 μL of clodronate, and we then evaluated the effects of the probiotics on RSV infection. RSV mRNA expression in lungs was examined using qPCR at 3 days after RSV infection (n=4). **g** FACS analysis of phosphorylated TBK1 (Ser172) in AMs at 24 h after RSV infection. **h** FACS analysis of phosphorylated IRF3 (Ser396) in AMs at 24 h after RSV infection. All results are expressed as the mean±SD (**a**–**f**). *P<0.05, **P<0.01, ***P<0.001 by Student's t test.

concentrations of SCFAs, including acetate, propionate, and butyrate, in feces and blood. SCFAs are important metabolites and rich products of gut bacteria metabolism and play a key role in multiple processes, such as anti-inflammatory, antiviral, and antibacterial effects [53]. A recent study reported that gut dysbiosis in influenza infection leads to decreased SCFAs, and supplementation with SCFAs (acetate) restores the killing activity of AMs to protect against bacterial superinfection [4]. A previous study showed that gut dysbiosis can exacerbate allergic lung inflammation through both T cell- and DC-dependent mechanisms that are inhibited by SCFAs [54]. These recent studies indicated that SCFAs play a role in modulating the lung immune response. More recently, a study demonstrated that SCFAs (acetate) promoted antiviral effects through the activation of the IFN-β response in pulmonary epithelial cells in RSV-infected mice and enhanced IFN-β secretion in A549 cells upon RSV infection [13]. Based on the anti-inflammatory and antiviral roles of SCFAs, we conclude that the effects of probiotics on lung injury, lung inflammation, and anti-RSV might be attributed to the elevated SCFA levels in RSV-infected mice. A previous study revealed that acetate supplementation could promote IFN-β secretion to defend against RSV infection [13]. AMs are the first line of cellular defense against respiratory viral infection by secreting IFN-β [47, 48]. In our study, the probiotic mixture significantly increased acetate-induced IFN-β expression in AMs. IFNAR1 block and AM depletion experiments confirmed the anti-RSV effects of the probiotic mixture through AM-derived IFNβ. Acetate supplementation and cohousing experiments further substantiated the importance of gut microbiota-derived SCFAs in the anti-RSV effects of the probiotic mixture. Although we have shown that SCFAs were responsible for the anti-RSV effects of the probiotics, some limitations still exist; for details, please see the Limitations of the Study section.

It is worth noting that we were the first to report the dysregulation of the lung microbiota in RSV-infected mice. In this study, we found that the diversity and composition of the lung microbiota were both changed, and the probiotic mixture significantly reversed lung dysbiosis by restoring diversity and dominant bacteria. A previous study showed that the dietary fermentable fiber content changed the composition of the gut and lung microbiota, particularly by decreasing the ratio of *Firmicutes* to *Bacteroidetes* [41], suggesting that SCFAs may modulate the lung microbiota. Similarly, our data showed that the dietary probiotic mixture reduced the *Firmicutes* to *Bacteroidetes* ratio. Therefore, we believe that the modulation of lung microbiota by the probiotic mixture may occur through SCFAs. However, our data are insufficient to validate SCFAs as solely responsible for the effects of the probiotic mixture on modulation of lung microbiota, and we will continue to explore this question in future studies.

The lung microbiota has been suggested to play several important roles in the development, regulation, and maintenance of healthy immune responses [17, 19]. Dysbiosis and the subsequent dysregulation of lung microbiota-related immunological processes affect the onset of disease in the lung [17, 19]. A previous study showed that *Corynebacterium* and *Lactobacillus* played a protective role in multiple respiratory viral infections; these bacteria induce macrophages to secrete IFN-β to defend against viral infections, suggesting that targeting *Corynebacterium* and *Lactobacillus* may be a promising approach for RSV therapy [23, 43]. In our study, we report, for the first time, that the levels of *Corynebacterium* and *Lactobacillus* were decreased in RSV-infected mice, and the probiotic mixture significantly elevated these bacteria, suggesting that the probiotic mixture promotes AM-mediated type I IFN production via *Corynebacterium* and *Lactobacillus*. A previous study showed that SCFAs are important carbon sources in *Corynebacterium* and *Lactobacillus* reproduction [44–46], and we suspect that increased *Corynebacterium* and *Lactobacillus* in probiotic mixture-treated mice may occur through SCFAs. The detailed mechanism will be further explored in the future.

In conclusion, the probiotic mixture protects against RSV-induced lung pathology by suppressing RSV infection and exerting an antiviral response via AMs.

The probiotic mixture promotes the AM secretion of IFN-β by gut microbiota-derived acetate and lung bacteria, including *Corynebacterium* and *Lactobacillus*. Our findings provide a microbiome-targeting therapeutic strategy and suggest the potential therapeutic value of probiotics in the treatment of RSV infection.

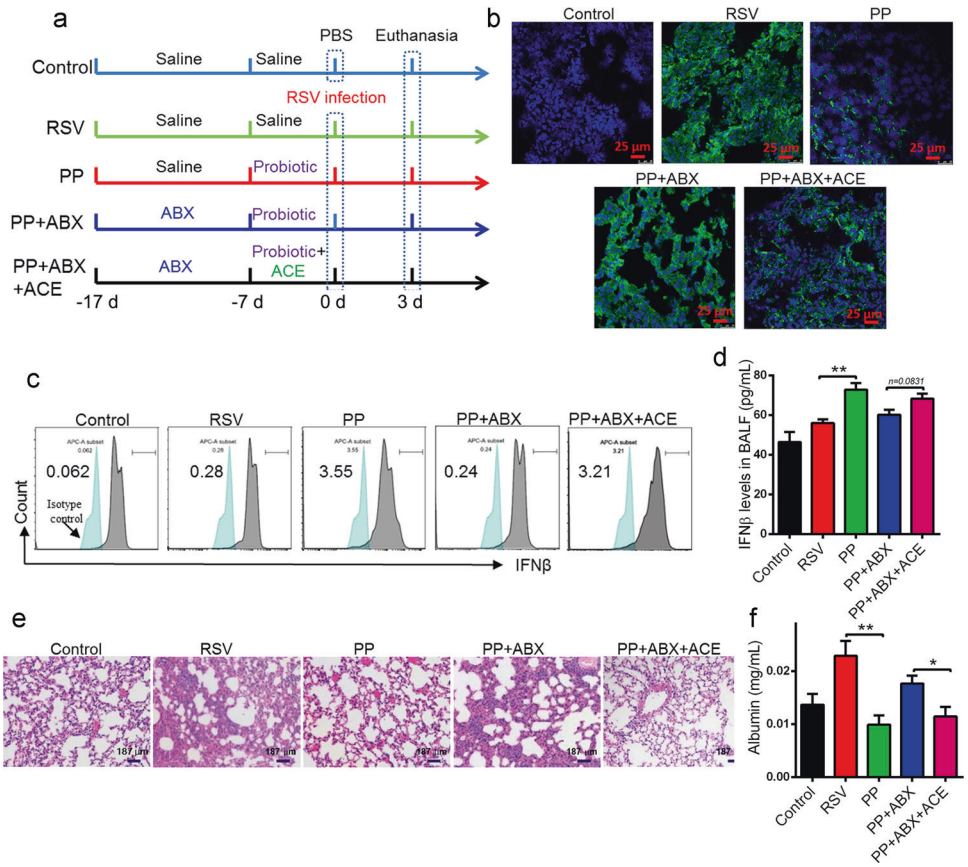

Fig. 7 The antiviral effects of probiotic pretreatment are mediated through acetate. a The experimental design. **b** RSV-F protein staining for evaluating the viral load in the lungs of mice using immunofluorescence at 3 days after RSV infection (n=4). Blue: DAPI; Green: RSV-F protein. **c** The expression of IFNβ in isolated AMs from all groups of mice was determined by FACS at 24 h after RSV infection (n=4). **d** The levels of IFNβ in BALF from all groups of mice were examined by ELISA at 24 h after RSV infection (n=4). **e** Representative H&E-stained lung tissue from mice showed histologic differences at 3 days after RSV infection (n=4). f The albumin level in BALF was determined at 3 days after RSV infection (n=4). All results are expressed as the mean±SD (**a**–**f**). *P<0.05, **P<0.01 by Student's t test.

Limitations of the study

Acetate can act through the G-protein-coupled receptors FFAR2 (formerly GPR43) and FFAR3 (formerly GPR41); [4] therefore, FFAR2$^{-/-}$ and FFAR3$^{-/-}$ mice should be used to further prove that acetate is responsible for the anti-RSV effects of probiotics. Moreover, we found that probiotics modulated the lung microbiota by SCFAs, but these results remained descriptive, and we failed to explore the detailed mechanism in this study.

ACKNOWLEDGEMENTS

This work was supported by the National Natural Science Foundation of China (81673412, 013038007001), Key R & D and promotion project of Henan Province (Science and technology tackling, Project No: 192102310431), the Jiangsu Key R&D Plan (Social Development) BE2019618, Six Talent Peaks in Jiangsu Province (YY-013), the Jiangsu Province TCM Science and Technology Development Plan Project (ZD201901), the Grant for Special Professors of Jiangsu (2015), a project funded by the Priority Academic Program Development of Jiangsu Higher Education Institutions (PAPD), and The Open Projects of the Discipline of Chinese Medicine of Nanjing University of Chinese Medicine Supported by the Subject of Academic priority discipline of Jiangsu Higher Education Institutions (ZYX03KF053).

AUTHOR CONTRIBUTIONS

ZGL and GMP conceived and designed the experiments. JJJ, QMS, DYN, QW, HZ, FFQ, QSW and SFL performed the experiments. ZGL and QMS analyzed the data. JJJ wrote the manuscript.

ADDITIONAL INFORMATION

The online version of this article (https://doi.org/10.1038/s41401-020-00573-5) contains supplementary material, which is available to authorized users.

Competing interests: The authors declare no competing interests.

REFERENCES

1. Li Y, Reeves RM, Wang X, Bassat Q, Brooks WA, Cohen C, et al. Global patterns in monthly activity of influenza virus, respiratory syncytial virus, parainfluenza virus, and metapneumovirus: a systematic analysis. Lancet Glob Health. 2019;7: e1031–e1045.
2. Groves HT, Cuthbertson L, James P, Moffatt MF, Cox MJ, Tregoning JS. Respiratory disease following viral lung infection alters the murine gut microbiota. Front Immunol. 2018;9:182.
3. Burgess SL, Leslie JL, Uddin MJ, Oakland DN, Gilchrist CA, Moreau GB, et al. Gut microbiome communication with bone marrow regulates susceptibility to amebiasis. J Clin Invest. 2020;130:4019–24.
4. Sencio V, Barthelemy A, Tavares LP, Machado MG, Soulard D, Cuinat C, et al. Gut Dysbiosis during influenza contributes to pulmonary pneumococcal superinfection through altered short-chain fatty acid production. Cell Rep. 2020; 30:2934–2947.e6.
5. Yildiz S, Mazel Sanchez B, Kandasamy M, Manicassamy B, Schmolke M. Influenza A virus infection impacts systemic microbiota dynamics and causes quantitative enteric dysbiosis. Microbiome. 2018;6:9.
6. Groves HT, Higham SL, Moffatt MF, Cox MJ, Tregoning JS. Respiratory viral infection alters the gut microbiota by inducing inappetence. mBio. 2020;11: e03236–19.

7. Dang AT, Marsland BJ. Microbes, metabolites, and the gut-lung axis. Mucosal Immunol. 2019;12:843–50.
8. Hagan T, Cortese M, Rouphael N, Boudreau C, Linde C, Maddur MS, et al. Antibiotics-driven gut microbiome perturbation alters immunity to vaccines in humans. Cell. 2019;178:1313–1328.e13.
9. Nemet I, Saha PP, Gupta N, Zhu W, Romano KA, Skye SM, et al. A Cardiovascular disease-linked gut microbial metabolite acts via adrenergic receptors. Cell. 2020; 180:862–877.e22.
10. Abt MC, Osborne LC, Monticelli LA, Doering TA, Alenghat T, Sonnenberg GF, et al. Commensal bacteria calibrate the activation threshold of innate antiviral immunity. Immunity. 2012;37:158–70.
11. Ganal SC, Sanos SL, Kallfass C, Oberle K, Johner C, Kirschning C, et al. Priming of natural killer cells by nonmucosal mononuclear phagocytes requires instructive signals from commensal microbiota. Immunity. 2012;37:171–86.
12. Winkler ES, Thackray LB. A long-distance relationship: the commensal gut microbiota and systemic viruses. Curr Opin Virol. 2019;37:44–51.
13. Antunes KH, Fachi JL, de Paula R, da Silva EF, Pral LP, Dos Santos AA, et al. Microbiota-derived acetate protects against respiratory syncytial virus infection through a GPR43-type 1 interferon response. Nat Commun. 2019;10:3273.
14. Swimm A, Giver CR, DeFilipp Z, Rangaraju S, Sharma A, Ulezko Antonova A, et al. Indoles derived from intestinal microbiota act via type I interferon signaling to limit graft-versus-host disease. Blood. 2018;132:2506–19.
15. Trompette A, Gollwitzer ES, Pattaroni C, Lopez-Mejia IC, Riva E, Pernot J, et al. Dietary fiber confers protection against Flu by shaping Ly6c(-) patrolling monocyte hematopoiesis and $CD8^+$ T cell metabolism. Immunity. 2018;48:992–1005.e8.
16. Yitbarek A, Taha Abdelaziz K, Hodgins DC, Read L, Nagy E, Weese JS, et al. Gut microbiota-mediated protection against influenza virus subtype H9N2 in chickens is associated with modulation of the innate responses. Sci Rep. 2018;8:13189.
17. Man WH, van Houten MA, Merelle ME, Vlieger AM, Chu M, Jansen NJG, et al. Bacterial and viral respiratory tract microbiota and host characteristics in children with lower respiratory tract infections: a matched case-control study. Lancet Respir Med. 2019;7:417–26.
18. Gollwitzer ES, Saglani S, Trompette A, Yadava K, Sherburn R, McCoy KD, et al. Lung microbiota promotes tolerance to allergens in neonates via PD-L1. Nat Med. 2014;20:642–7.
19. Yang D, Chen X, Wang J, Lou Q, Lou Y, Li L, et al. Dysregulated Lung commensal bacteria drive interleukin-17B production to promote pulmonary fibrosis through their outer membrane vesicles. Immunity 2019;50:692–706.e7.
20. Dumas A, Bernard L, Poquet Y, Lugo-Villarino G, Neyrolles O. The role of the lung microbiota and the gut-lung axis in respiratory infectious diseases. Cell Microbiol. 2018;20:e12966.
21. Marsh RL, Smith Vaughan HC, Chen ACH, Marchant JM, Yerkovich ST, Gibson PG, et al. Multiple respiratory microbiota profiles are associated with lower airway inflammation in children with protracted bacterial bronchitis. Chest 2019;155:778–86.
22. Stewart CJ, Mansbach JM, Ajami NJ, Petrosino JF, Zhu Z, Liang L, et al. Serum metabolome is associated with nasopharyngeal microbiota and disease severity among infants with bronchiolitis. J Infect Dis. 2019;219:2005–14.
23. Kanmani P, Clua P, Vizoso Pinto MG, Rodriguez C, Alvarez S, Melnikov V, et al. Respiratory commensal bacteria *Corynebacterium pseudodiphtheriticum* improves resistance of infant mice to respiratory dyncytial virus and *Streptococcus pneumoniae* duperinfection. Front Microbiol. 2017;8:1613.
24. Korpela K, Salonen A, Vepsalainen O, Suomalainen M, Kolmeder C, Varjosalo M, et al. Probiotic supplementation restores normal microbiota composition and function in antibiotic-treated and in caesarean-born infants. Microbiome. 2018;6:182.
25. Suez J, Zmora N, Segal E, Elinav E. The pros, cons, and many unknowns of probiotics. Nat Med. 2019;25:716–29.
26. van den Elsen LWJ, Tims S, Jones AM, Stewart A, Stahl B, Garssen J, et al. Prebiotic oligosaccharides in early life alter gut microbiome development in male mice while supporting influenza vaccination responses. Benef Microbes. 2019;10:279–91.
27. Kumova OK, Fike AJ, Thayer JL, Nguyen LT, Mell JC, Pascasio J, et al. Lung transcriptional unresponsiveness and loss of early influenza virus control in infected neonates is prevented by intranasal Lactobacillus rhamnosus GG. PLoS Pathog. 2019;15:e1008072.
28. Vlasova AN, Shao L, Kandasamy S, Fischer DD, Rauf A, Langel SN, et al. Escherichia coli Nissle 1917 protects gnotobiotic pigs against human rotavirus by modulating pDC and NK-cell responses. Eur J Immunol. 2016;46:2426–37.
29. De Angelis M, Scagnolari C, Oliva A, Cavallari EN, Celani L, Santinelli L, et al. Short-term probiotic administration increases fecal-anti candida activity in healthy dbjects. Microorganisms. 2019;7:162.
30. Li J, Sung CY, Lee N, Ni Y, Pihlajamaki J, Panagiotou G, et al. Probiotics modulated gut microbiota suppresses hepatocellular carcinoma growth in mice. Proc Natl Acad Sci USA. 2016;113:E1306–15.
31. Kolli D, Gupta MR, Sbrana E, Velayutham TS, Chao H, Casola A, et al. Alveolar macrophages contribute to the pathogenesis of human metapneumovirus infection while protecting against respiratory syncytial virus infection. Am J Respir Cell Mol Biol. 2014;51:502–15.
32. Shen C, Zhang Z, Xie T, Xu J, Yan J, Kang A, et al. Jinxin oral liquid inhibits human respiratory syncytial virus-induced excessive inflammation associated with blockade of the NLRP3/ASC/Caspase-1 pathway. Biomed Pharmacother. 2018; 103:1376–83.
33. Dong Y, Yan H, Zhao X, Lin R, Lin L, Ding Y, et al. Gu-Ben-Fang-Xiao decoction ameliorated murine asthma in remission stage by modulating microbiota-acetate-Tregs axis. Front Pharmacol. 2020;11:549.
34. Zhang X, Goncalves R, Mosser DM. The isolation and characterization of murine macrophages. Curr Protoc Immunol. 2008 Nov;Chapter 14:Unit 14.1.
35. Haeberle HA, Takizawa R, Casola A, Brasier AR, Dieterich HJ, Van Rooijen N, et al. Respiratory syncytial virus-induced activation of nuclear factor-kappaB in the lung involves alveolar macrophages and toll-like receptor 4-dependent pathways. J Infect Dis. 2002;186:1199–206.
36. Amato KR, Yeoman CJ, Kent A, Righini N, Carbonero F, Estrada A, et al. Habitat degradation impacts black howler monkey (Alouatta pigra) gastrointestinal microbiomes. ISME J. 2013;7:1344–53.
37. Schloss PD, Westcott SL, Ryabin T, Hall JR, Hartmann M, Hollister EB, et al. Introducing mothur: open-source, platform-independent, community-supported software for describing and comparing microbial communities. Appl Environ Microbiol. 2009;75:7537–41.
38. Ji J, Ge X, Chen Y, Zhu B, Wu Q, Zhang J, et al. Daphnetin ameliorates experimental colitis by modulating microbiota composition and Treg/Th17 balance. FASEB J. 2019;33:9308–22.
39. Barcik W, Boutin RCT, Sokolowska M, Finlay BB. The role of lung and gut microbiota in the pathology of asthma. Immunity 2020;52:241–55.
40. Shenoy MK, Fadrosh DW, Lin DL, Worodria W, Byanyima P, Musisi E, et al. Gut microbiota in HIV-pneumonia patients is related to peripheral CD4 counts, lung microbiota, and in vitro macrophage dysfunction. Microbiome 2019;7:37. Mar 11
41. Trompette A, Gollwitzer ES, Yadava K, Sichelstiel AK, Sprenger N, Ngom Bru C, et al. Gut microbiota metabolism of dietary fiber influences allergic airway disease and hematopoiesis. Nat Med. 2014;20:159–66.
42. Nagre N, Cong X, Pearson AC, Zhao X. Alveolar macrophage phagocytosis and bacteria clearance in mice. J Vis Exp. 2019;10.3791/59088.
43. Lee H, Ko G. Antiviral effect of vitamin A on norovirus infection via modulation of the gut microbiome. Sci Rep. 2016;6:25835.
44. Huser AT, Becker A, Brune I, Dondrup M, Kalinowski J, Plassmeier J, et al. Development of a Corynebacterium glutamicum DNA microarray and validation by genome-wide expression profiling during growth with propionate as carbon source. J Biotechnol. 2003;106:269–86.
45. Gerstmeir R, Wendisch VF, Schnicke S, Ruan H, Farwick M, Reinscheid D, et al. Acetate metabolism and its regulation in Corynebacterium glutamicum. J Biotechnol. 2003; 104:99–122.
46. Wendisch VF, Spies M, Reinscheid DJ, Schnicke S, Sahm H, Eikmanns BJ. Regulation of acetate metabolism in Corynebacterium glutamicum: transcriptional control of the isocitrate lyase and malate synthase genes. Arch Microbiol. 1997;168:262–9.
47. Grunwell JR, Yeligar SM, Stephenson S, Ping XD, Gauthier TW, Fitzpatrick AM, et al. TGF-beta1 suppresses the type I IFN response and induces mitochondrial dysfunction in alveolar macrophages. J Immunol. 2018;200:2115–28.
48. Goritzka M, Makris S, Kausar F, Durant LR, Pereira C, Kumagai Y, et al. Alveolar macrophage-derived type I interferons orchestrate innate immunity to RSV through recruitment of antiviral monocytes. J Exp Med. 2015;212:699–714.
49. Steed AL, Christophi GP, Kaiko GE, Sun L, Goodwin VM, Jain U, et al. The microbial metabolite desaminotyrosine protects from influenza through type I interferon. Science. 2017;357:498–502.
50. Ye W, Chew M, Hou J, Lai F, Leopold SJ, Loo HL, et al. Microvesicles from malaria-infected red blood cells activate natural killer cells via MDA5 pathway. PLoS Pathog. 2018;14:e1007298.
51. Marr N, Turvey SE, Grandvaux N. Pathogen recognition receptor crosstalk in respiratory syncytial virus sensing: a host and cell type perspective. Trends Microbiol. 2013;21:568–74.
52. Kim D, Hofstaedter CE, Zhao C, Mattei L, Tanes C, Clarke E, et al. Optimizing methods and dodging pitfalls in microbiome research. Microbiome. 2017;5:52.
53. Bachem A, Makhlouf C, Binger KJ, de Souza DP, Tull D, Hochheiser K, et al. Microbiota-derived short-chain fatty acids promote the memory potential of antigen-activated $CD8^+$ T cells. Immunity. 2019;51:285–97.e5.
54. Cait A, Hughes MR, Antignano F, Cait J, Dimitriu PA, Maas KR, et al. Microbiome-driven allergic lung inflammation is ameliorated by short-chain fatty acids. Mucosal Immunol. 2018;11:785–95.